Add-In – non-Darcy flow

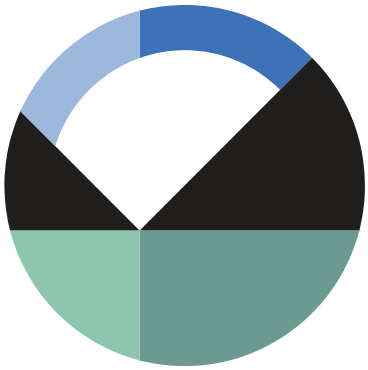

GEOSLOPE International Ltd. | www.geoslope.com

1200, 700 - 6th Ave SW, Calgary, AB, Canada T2P 0T8
Main: +1 403 269 2002 | Fax: +1 888 463 2239

Introduction

The mathematical description of mass transfer hinges on the principle of mass conservation and the phenomenological equation that describes flow in porous media. In most studies, groundwater flow is assumed to obey Darcy's law. This assumption is only valid at low fluid velocities, where viscous effects prevail. At larger velocities, both viscous and inertial effects are present and a term must be added to the Darcy equation. The resulting quadratic equation is known as the Darcy-Forchheimer equation.

The objective of this example is to verify the Darcy-Forchheimer formulation against an analytical solution for transient, one-dimensional, non-Darcy flow in a saturated aquifer. The verification exercise lends credibility to the use of the Darcy-Forchheimer formulation for problems involving two and three-dimensional flow fields in more complicated hydrogeological settings.

Background

Darcy's law is the simplest model for describing groundwater flow. Initially derived from experimental data, the law states that the superficial flux (or apparent fluid velocity) is a linear function of the hydraulic gradient, such that:

$$\nabla h = -\frac{q_w}{k_w} \qquad \text{Equation 1}$$

where h is the total head, q_w is the superficial flux vector, and k_w is the hydraulic conductivity. As previous noted, this relation is only valid at small values of superficial flux. At larger values, the fluid resists changes in velocity and direction as it encounters the soil particles, and the linear function transitions into a nonlinear relationship. In this transitional (laminar to turbulent), or non-Darcy flow, the appropriate form of the momentum equation can be written as follows (Joseph et al., 1982):

$$\nabla h = -\frac{q_w}{k_w} - c_F \sqrt{\frac{\rho_w}{k_w g \mu_w}} |q_w| q_w \qquad \text{Equation 2}$$

where $|q_w|$ is the Euclidean norm of the superficial flux vector, c_F is the dimensionless form-drag constant, ρ_w is the fluid density, g is the gravity vector, and μ_w is the dynamic viscosity of the fluid. The first term on the right-hand side of this quadratic equation is Darcy's viscous term whereas the second term is Forchheimer's inertial term. The nonlinear nature of this equation can be relegated to an apparent hydraulic conductivity term by rearranging the equation as follows:

$$q_w = -k_{w,a} \nabla h \qquad \text{Equation 3}$$

where $k_{w,a} = k_w \Big/ \left(1 + c_F \sqrt{k_w} \sqrt{\frac{\rho_w}{g \mu_w}} |q_w|\right)$ is the apparent hydraulic conductivity. The apparent hydraulic conductivity can be expressed in different forms by using the Forchheimer coefficient, $\beta = c_F \Big/ \sqrt{\frac{k_w \mu_w}{\rho_w g}}$, or the Forchheimer number, $F = \beta k_w q_w / g$ (Ruth and Ma, 1992; Ma and Ruth, 1993). As pointed out by Knupp and Lage (1995), the apparent hydraulic conductivity can also be expressed in terms of total head by solving the quadratic equation that results from inserting equation (3) into equation (2), and taking the positive root:

$$k_{w,a} = \frac{-1 + \sqrt{1 + 4 c_F k_w^{3/2} \sqrt{\frac{\rho_w}{g \mu_w}} |\nabla h|}}{2 c_F \sqrt{k_w} \sqrt{\frac{\rho_w}{g \mu_w}} |\nabla h|} \qquad \text{Equation 4}$$

Although this expression may seem daunting, it is of great practical importance as it expresses the nonlinear aspect of flow in terms of the independent variable. It must be noted that this expression adequately describes groundwater flow as long as the fluxes remain low to intermediate (Wu et al., 2011). Table 1 provides an indication of expected parameter values for a number of different uniformly-graded cohesionless soils.

Table 1. Physical and hydraulic properties of different cohesionless soils at 20°C.

Material	Source	D [m]	k_w [m/s]	c_F
Coarse sand	Ahmed and Sunada (1969)	0.0026	0.0215	0.76
Fine gravel	Bordier and Zimmer (2000)	0.1000 - 0.1400	0.7937	0.10
Coarse gravel	Dudgeon (1966)	0.0250	3.9089	0.75

Cobbles	Dudgeon (1966)	0.0840	19.9354	0.21
Cobbles	Zhang et al. (2013)	0.1400	78.1782	0.18
Cobbles	Zhang et al. (2013)	0.1740	178.8327	0.21
Cobbles	Zhang et al. (2013)	0.2640	258.9653	0.20

In this case, the partial differential equation for groundwater flow is obtained by introducing the Darcy-Forchheimer equation into the equation of mass conservation, such that:

$$\rho_w \frac{\partial\left(V_w/V_o\right)}{\partial t} + \frac{V_w \partial \rho_w}{V_o\ \partial t} - \nabla \cdot \left(\rho_w k_{w,a} \nabla h\right) = 0 \qquad \text{Equation 5}$$

where V_w is the volume of fluid, V_o is the control volume, and t is the time. Under saturated conditions, the time derivative of the ratio of fluid volume to control volume is equal to the time derivative of the constitutive equation of the fluid, such that $\partial\left(V_w/V_o\right)/\partial t = -\beta_s \partial \sigma'/\partial t$ where β_s is the soil structure compressibility, and σ' is the effective stress. Assuming that the external load remains constant, the equation reduces to $\partial\left(V_w/V_o\right)/\partial t = \beta_s \partial u_w/\partial t$ where u_w is the pore-water pressure. Introducing this expression into equation (5), reformulating the time derivative of the fluid density in terms of its compressibility at constant temperature, $\partial \rho_w/\partial t = \rho_w \beta_w \partial u_w/\partial t$, and recognizing that the pore-water pressure is a function of total head, $u_w = \rho_w g(h - y)$ where y is the elevation, the equation reduces to:

$$\rho_w g\left(\frac{V_w}{V_o}\beta_w + \beta_s\right)\frac{\partial h}{\partial t} - \nabla \cdot \left(k_{w,a} \nabla h\right) = 0 \qquad \text{Equation 6}$$

or then again:

$$S_s \frac{\partial h}{\partial t} - \nabla \cdot \left(k_{w,a} \nabla h\right) = 0 \qquad \text{Equation 7}$$

where $S_s = \rho_w g\left(\frac{V_w}{V_o}\beta_w + \beta_s\right)$ is the specific storage. These equations differ from those generally used to describe groundwater flow only by the use of an apparent hydraulic conductivity. It therefore follows that non-Darcy flow can be implemented into GeoStudio by simply replacing the Hydraulic Conductivity Function with an Add-In.

For the sake of completeness, it must be noted that the Reynolds number provides a means of quantifying the effect of the inertial forces. Although initially derived for flow in conduits, the following form of the Reynolds number is adapted to describe non-Darcy flow in porous media:

$$R_e = \frac{\rho_w D q_w}{\mu_w} \qquad \text{Equation 8}$$

where D is the particle diameter, and q_w is the superficial flux. Although there is no widely accepted criterion for the onset of non-Darcy flow, it most certainly occurs as the Reynolds number approaches 100 (Zeng and Grigg, 2006).

Numerical Simulation

In this example, the ability of the model is evaluated with a benchmark problem for non-Darcy flow in a saturated and homogeneous confined aquifer. As shown in Figure 1, the aquifer is assumed to lay between two rivers with variable water levels. The length, L, and thickness, B, of the aquifer are considered equal to 3000 and 10 m, respectively. Although the total head is initially constant at h_o = 10 m, it suddenly rises to 11 m on the left-hand side of the aquifer and remains constant on the right-hand side. The specific storage of the aquifer is equal to 0.02 m^{-1}, and the soil structure compressibility is equal to $S_s/(\rho_w g) - \frac{V_w}{V_o}\beta_w$ = 0.002 kPa^{-1}. The fluid density and dynamic viscosity are computed at 20°C, and thus equal to 998.20 kg/m^3 and 1.00×10^{-3} kg/(m s), respectively. The hydraulic conductivity of the

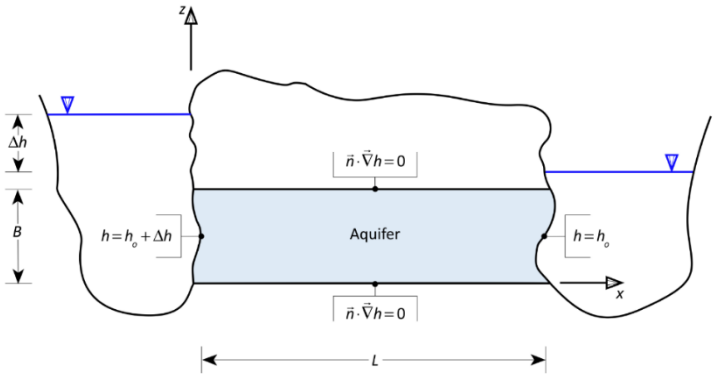

aquifer is equal to 20 m/s whereas the dimensionless form-drag constant is equal to 0.21. The remaining parameter inputs can be viewed within the example file.

Figure 1. Schematic representation of the confined aquifer with boundary conditions.

Although saturated, the hydraulic properties of the aquifer are described by the Van Genuchten Non-Darcy Flow Add-In. Access to the Add-In functions is provided through the Add-In Function Type menu

in the pop-up window of each function of the Saturated/Unsaturated Material Model. The inputs of the volumetric water content Add-In function are soil structure compressibility, saturated water content, residual water content, and curve-fitting parameters *alpha* and *n*. The inputs of the hydraulic conductivity Add-In function are saturated hydraulic conductivity, saturated water content, residual water content, curve-fitting parameters *alpha*, *n*, and *l*, as well as the form-drag constant and the temperature.

Results and Discussion

Figure 2 shows the relationship between the superficial flux, the hydraulic gradient, the apparent hydraulic conductivity, and the Reynolds number for the confined aquifer problem. Figure 2a shows that the linear relation between the superficial flux and the gradient rapidly transforms into a nonlinear relation as the superficial flux increases, and the inertial forces become important. As a result, the apparent hydraulic conductivity decreases to 1.25 m/s as the superficial flux reaches 0.05 m/s (refer to Figure 2b). Assuming that the mean particle diameter is equal to 0.1 m, Figure 2c shows that the Reynolds number approaches the critical value of 100 as the superficial flux reaches 0.001 m/s, which corresponds to a hydraulic gradient of 0.0001 m/m. This value corresponds very well to the hydraulic gradient at which the relation between the superficial flux and the gradient becomes nonlinear, and inertial forces start to prevail (refer to Figure 2a).

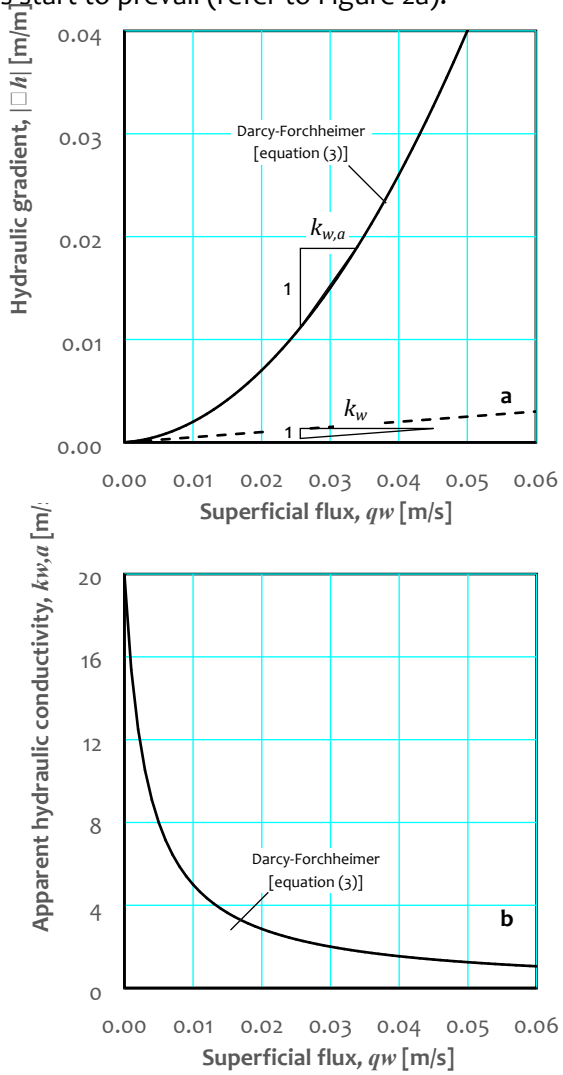

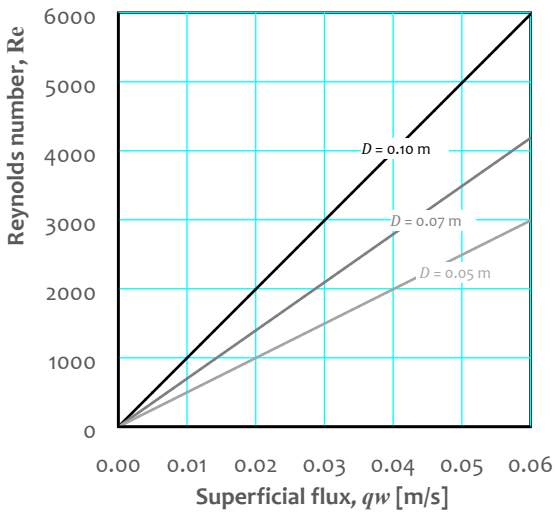

Figure 2. Flow configuration in the confined aquifer problem. (a) Relationdhip between the superficial flux and the hydraulic gradient. (b) Relationship between the superficial flux and the apparent hydraulic conduc-tivity. (c) Reynolds number at different mean particle diameters.

Figure 3 shows the evolution of total head in the confined aquifer. As expected, the increase in total head at the left-hand side boundary produces groundwater flow, which slowly increases the total head throughout the aquifer. The total head continues to increase with time until steady-state conditions are reached. The numerical results after 42, 99 and 504 s are in close agreement with the analytical

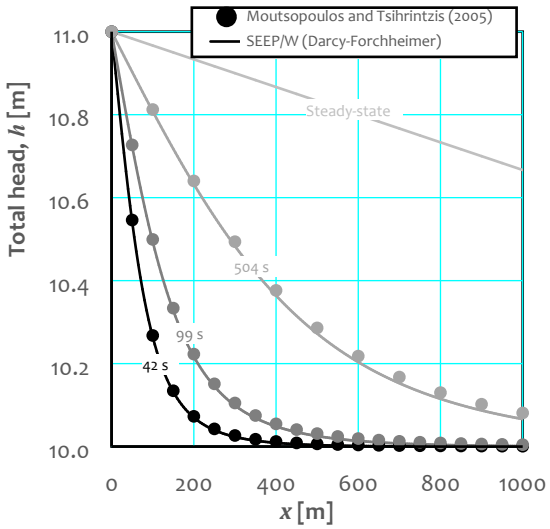

solution provided by Moutsopoulos and Tsihrintzis (2005).

Figure 3. Total head in the confined aquifer problem.

Figure 4 shows that the apparent hydraulic conductivity is much lower at the left-hand side boundary, where superficial fluxes are highest. The apparent hydraulic conductivity continues to evolve until steady-state conditions are reached. Under these conditions, the apparent hydraulic conductivity is equal to 10 m/s, which is two times smaller than the saturated hydraulic conductivity. The flow rate through the aquifer is therefore much smaller than that which would be computed with Darcy's law.

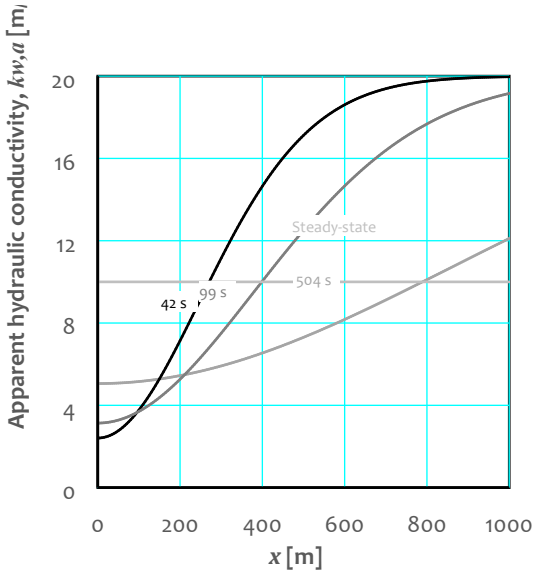

Figure 4. Apparent hydraulic conductivity in the confined aquifer.

Summary and Conclusions

The objective of this example was to demonstrate the ability to solve a non-Darcy flow problem in SEEP/W. Given that the partial differential equation for non-Darcy flow differs only by the use of an apparent hydraulic conductivity, the model was implemented into the software by simply replacing the hydraulic conductivity function with an Add-In. In so doing, the apparent hydraulic conductivity was explicitly computed from known values of hydraulic gradient. The capabilities of the model were assessed by comparing the numerical results to those of an analytical solution for transient non-Darcy flow in a confined aquifer. The results were shown to be in close agreement with those of the analytical solution at various points in time.

References

Ahmed, N., and Sunada, D.K. 1969. Nonlinear flow in porous media. Proceedings of the American Society of Civil Engineers – Journal of the Hydraulics Division, 95 (6), 1847-1857.

Bordier, C., and Zimmer, D. 2000. Drainage equations and non-Darcian modelling in coarse porous media or geosynthetic materials. Journal of Hydrology, 228 (3-4), 174-187.

Dudgeon, C.R. 1966. An experimental study of flow of water through coarse granular media. La Houille Blanche, 7, 785-801.

Joseph, D.D., Nield, D.A., and Papanicolaou, G. 1982. Nonlinear equation governing flow in a saturated porous media. Water Resources Research, 18 (4), 1049-1052.

Knupp, P.M., and Lage, J.L. 1995. Generalization of the Forchheimer-extended Darcy flow model to the tensor permeability case via variational principle. Journal of Fluid Mechanics 299: 97-104.

Ma, H., and Ruth, D. 1993. The microscopic analysis of high Forchheimer number flow in porous media. Transport in Porous media, 13 (2), 139-160.

Moutsopoulos, K.N., and Tsihrintzis, V.A. 2005. Approximate analytical solutions of the Forchheimer equation. Journal of Hydrology, 309 (1-4), 93-103.

Ruth, D., and Ma, H. 1992. On the derivation of the Forchheimer equation by means of the averaging theorem. Transport in Porous media, 7 (3), 255-264.

Wu, Y.-S., Lai, B., and Miskimins, J.L. 2011. Simulation of non-Darcy porous media flow according to the Barree and Conway model. The Journal of Computational Multiphase Flows, 3 (2), 107-122.

Zeng, Z., and Grigg, R. 2006. A criterion for non-Darcy flow in porous media. Transport in Porous media, 63 (1), 57-69.

Zhang, M., Lai, Y., Li, D., Chen, W., and Tong, G. 2013. Experimental study on ventilation characteristics of a concrete-sphere layer and a crushed-rock layer. International Journal of Heat and Mass Transfer, 59, 407-413.